Site preference and thermodynamic properties of $R_3Ni_{13-x}Co_xB_2$ (R=Y, Nd and Sm)*

Qian Ping(钱 萍)†, Liu Jiu-Li(刘九丽), Shen Jiang(申 江),
Bai Li-Jun(白丽君), Ran Qiong(冉 琼), and Wang Yun-Liang(王云良)

Institute of Applied Physics, Beijing University of Science and Technology, Beijing 100083, *China*

(Received 29 March 2010; revised manuscript received 3 June 2010)

This paper investigates the structural stability of intermetallics $R_3Ni_{13-x}Co_xB_2$ (R=Y, Nd and Sm) with $Nd_3Ni_{13}B_2$-type structure and the site preferences of the transition element Co by using a series of interatomic pair potentials. The space group remains unchanged upon substitution of Co for Ni in $R_3Ni_{13-x}Co_xB_2$ and the calculated lattice constants are found to agree with reports in literatures. The calculated cohesive energy curves show that Co atoms substitute for Ni with a strong preference for the 3g sites and the order of site preference is 3g, 4h and 6i. Moreover, the total and partial phonon densities of states are first evaluated for the $R_3Ni_{13}B_2$ compounds with the hexagonal $Nd_3Ni_{13}B_2$-type structure.

Keywords: interatomic potentials, site preference, crystal structure, lattice inversion

PACC: 6000, 6155, 3420, 8200W

1. Introduction

During the past few years, rare-earth-transition-metal intermetallic compounds have been widely investigated due to their potential as permanent magnets.[1−5] At present, research on high temperature performing magnets is of current interest. In this respect $SmCo_5$ shows excellent intrinsic magnetic properties and high attainable coercivity,[6,7] therefore, due to the richness of different phases it is a logic development to study boron derivatives of the RCo_5 series. The series formally denoted by $R_{m+n}T_{5m+3n}$+B_{2n} have attracted a particular interes.[8−18] The intermetallic compounds in the $R_{m+n}T_{5m+3n} + B_{2n}$ series, where T=Co or Ni, crystallize in layered structures (with space group symmetry $P6/mmm$), consisting of intergrown stacks of m $CaCu_5$-type slabs and n $CeCo_3B_2$-type slabs.[19] In particular, the 3:13:2 ($m = 2$, $n = 1$) consist of two 1:5 slabs stacked between 1:3:2 slabs. In theoretical research, Chen *et al.* have performed studies on the structural properties for the compounds of 1:5-type and their derivative compounds[20−25] from the viewpoint of energy. The method combining interatomic potentials with different crystal structures is a shortcut but effective way to investigate the structural stability and the site preference. It is accepted that the local atomic environment determines if the energy of a compound is low enough to form a compound with a certain structure. In the $R_{m+n}T_{5m+3n}B_{2n}$ series, the structural properties of the $R_2Co_7B_3$ series (for $m = 1$ and $n = 3$) with the $Ce_2Co_7B_3$-type structure had been reported in our previous work.[26] As a continuation of the systematic research, this work is focused on the member of the series with $m = 2$, $n = 1$ ($R_3T_{13}B_2$). Particular interest is devoted to the lattice vibrations of these intermetallic compounds with the hexagonal $Nd_3Ni_{13}B_2$-type structure. The purpose of the present work is to give some description of some properties such as phase stability, site preference, and Debye temperature of the $R_3Ni_{13-x}Co_xB_2$ (R=Y, Nd and Sm) series of compounds.

2. Calculational method

Since the mid 1990s, Chen's inversion theorem has been developed a rigorous and concise approach to obtain the interatomic pair potential based on the cohesive energy curves.[27,28] And it has been applied successfully to study the site preference of ternary additions in Ni_3Al and Fe_3Al,[29,30] the phase stabil-

*Project supported by the National Basic Research Program of China (Grant No. 2006CB605101) and the National Natural Science Foundation of China (Grant No. 50971024).

†Corresponding author. E-mail: qianping@ustb.edu.cn

© 2010 Chinese Physical Society and IOP Publishing Ltd

ity of $R\mathrm{Fe}_{12-x}T_x$,[20] $RM_{13-x}T_x$,[21] $R_2\mathrm{Co}_{17-x}\mathrm{Mn}_x$[22] and $R_3M_{29-x}T_x$[23,24] (R=rare earth; M=Fe, Co; T = transition metals), the lattice dynamics[25] and so on. These studies provide a strong foundation of and confidence in the method for application to the problem of studying many properties in intermetallic compounds. It is the structural complexity and particularly, the difficulties in acquiring potentials of rare-earth compounds which frustrate attempts to adopt this method. A detailed introduction to the lattice inversion method and the potential acquisition have been reported in our earlier papers,[22,26] where the relevant references can be found. Here, only some parameters of the potentials are shown in Fig. 1.

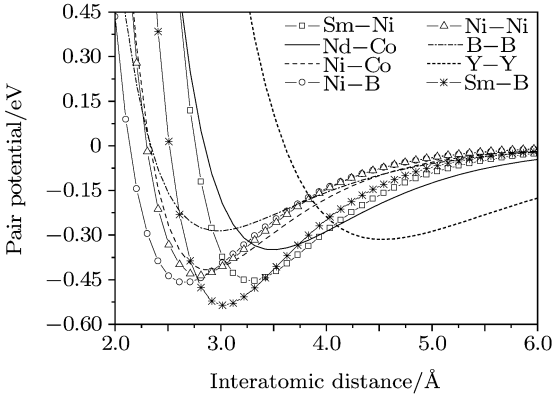


Fig. 1. Some important potentials of R–Co–Ni–B system (1 Å=0.1 nm).

3. Phase stability and Site preference of $R_3\mathrm{Ni}_{13-x}\mathrm{Co}_x\mathrm{B}_3$

The $R_3\mathrm{Ni}_{13-x}\mathrm{Co}_x\mathrm{B}_2$ (R=Y, Nd and Sm) crystallize in the hexagonal system with an $\mathrm{Nd}_3\mathrm{Ni}_{13}\mathrm{B}_2$-type structure in which the 3d metal atoms are located at the 6i, 4h and 3g symmetry sites of space group $P6_3/mmc$. Rare earth atoms are most reasonably placed at 2e and 1a sites and B at the 2c site. Based on any existing experimental structure close to $\mathrm{Nd}_3\mathrm{Ni}_{13}\mathrm{B}_2$ type with the $P6_3/mmc$ space group, for example, the atom position and symmetry of Refs. [16] and [17], initial $R_3\mathrm{Ni}_{13}\mathrm{B}_2$ structure is constructed within Accelrys Cerius 2 modeling software. Then, energy minimization is carried out by using the conjugate-gradient method on the basis of calculated *ab initio* effective pair potentials obtained through Chen's lattice inversion method.

In the calculation, the structural stability of the intermetallic compounds is judged by energy minimum. The calculation unit of $R_3\mathrm{Ni}_{13-x}\mathrm{Co}_x\mathrm{B}_2$ is a 5×5×5 cell (2250 atoms in total) expanded from the hexagonal $\mathrm{Nd}_3\mathrm{Ni}_{13}\mathrm{B}_2$-type unit cell. In the process, firstly we substitute Co atoms for Ni in each site of ternary $R_3\mathrm{Ni}_{13}\mathrm{B}_2$ compounds with different concentrations. Then the energy minimization method is applied to relax the quaternary system under the interaction of the potentials. Thus the average energy of the final structure can be investigated and compared. In order to quantitatively evaluate the substitution behaviour of alloying elements, we utilize the pair potentials to calculate the cohesive energies of different samples containing the same amount of quaternary additions, and then do the average. We adopt 30 samples for each case, in which the equivalent sites are randomly occupied by the Co atoms. Figure 2 shows

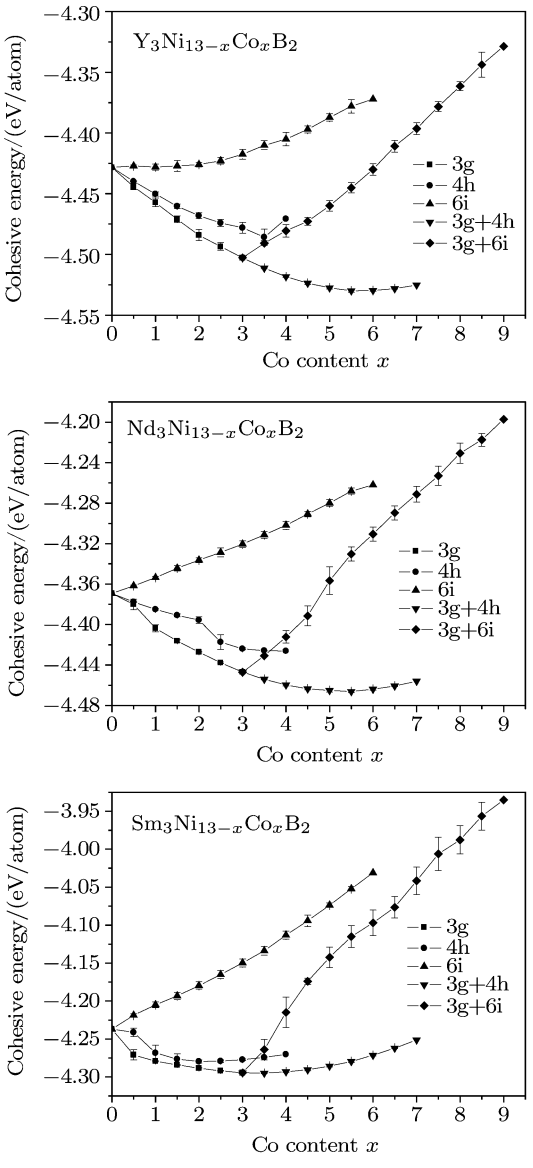


Fig. 2. Calculated cohesive energy of $R_3\mathrm{Ni}_{13-x}\mathrm{Co}_x\mathrm{B}_2$ as a function of the Co content.

that the calculated average energy of $R_3Ni_{13-x}Co_xB_2$ with $Nd_3Ni_{13}B_2$-type structure as a function of the Co content. It is found in Fig. 2 that the amount of cohesive energy changes is correlated with the content of Co atoms and various Ni crystallographic sites. The substitution of quaternary elements Co for Ni at the 4h and 3g sites decrease the cohesive energy of $R_3Ni_{13-x}Co_xB_2$, and thus stabilizes its structure of $Nd_3Ni_{13}B_2$-type. When the Co atoms occupy the 3g sites, the $R_3Ni_{13-x}Co_xB_2$ have the lowest energy for $x < 3$. So, in the calculation, when $x < 3$, Co atoms should prefer the 3g site of these compounds. In the composition range $x > 3$, three Co atoms have already occupied all the 3g sites based on the above analysis. So the remaining Co atoms can only occupy the 4h or 6i sites. The calculated cohesive energy is also shown in Fig. 2 when Co atoms occupy the 3g+4h and 3g+6i sites, respectively. The cohesive energy decreases with Co atoms entering into the 3g+4h sites and it increases with Co atoms entering into the 3g+6i sites. So when $x > 3$, Co atoms occupy the 4h sites besides three Co atoms occupying the 3g sites. Thus, from Fig. 2 it is easy to conclude that the Co atoms prefer the 3g site and the order of site preference is 3g, 4h and 6i.

With the same potentials, we also calculated the equilibrium lattice constant of the $R_3Ni_{13-x}Co_xB_2$ (R=Y, Nd and Sm) series of compounds. The results in Table 1 indicate that the present calculations are in agreement with the experimental data.[16−18] The largest deviation of a is 2.68 % while that of c is 5.03%. Our calculation assumes that $R_3Ni_{13-x}Co_xB_2$ has a relatively perfect periodic crystal structure, and Co atoms occupy the 3g sites for $x < 3$ or three Co atoms entirely distribute over the 3g sites for $x > 3$. These assumptions may result in a deviation of the calculations from the experimental data. Moreover, the trend of variation of the lattice constant as x changes is almost the same with the experimental reports.[16,17] That means the applicability of the present *ab initio* interatomic potentials is well proved by demonstrations.

Table 1. Comparison of calculated and experimental[16−18] lattice parameters.

compounds	a			c		
	Cal./Å	Exp./Å	Err./%	Cal./Å	Exp./Å	Err./%
$Y_3Ni_{13}B_2$	4.8605	4.9579[a]	1.96	11.4581	10.9141[a]	4.98
$Y_3Ni_{12}CoB_2$	4.8837	4.9585[a]	1.51	11.4378	10.9059[a]	4.88
$Y_3Ni_{10}Co_3B_2$	4.8968	4.9597[a]	1.27	11.4285	10.8930[a]	4.92
$Y_3Ni_8Co_5B_2$	4.9139	4.9661[a]	1.05	11.4106	10.8867[a]	4.81
$Y_3Ni_8Co_5B_2$ (503 K)	4.9301			11.4396		
$Nd_3Ni_{13}B_2$	5.0769	5.0255[b]	1.02	11.4834	10.9590[b]	4.79
$Nd_3Ni_7Co_6B_2$	5.1322	5.0476[b]	1.68	11.4435	10.9150[b]	4.84
$Nd_3Ni_{10}Co_3B_2$ (100 K)	4.9592	5.0049[c]	0.91	11.4006	10.8671[c]	4.91
$Nd_3Co_{13}B_2$ (295 K)	5.0286	5.1024[c]	1.45	11.4201	10.8770[c]	4.99
$Nd_3Co_{13}B_2$ (503 K)	5.1023	5.1160[c]	2.68	11.4533	10.9050[c]	5.03
$Sm_3Ni_{13}B_2$	5.0523			11.5125		
$Sm_3Ni_{12}CoB_2$ (295 K)	5.0666			11.5303		
$Sm_3Ni_{10}Co_3B_2$	5.0962			11.4918		
$Sm_3Ni_8Co_5B_2$ (503 K)	5.1214			11.5532		

[a] Reference [16], [b] reference [17], [c] reference [18].

The stability of $R_3Ni_{13-x}Co_xB_2$ (R=Y, Nd and Sm) with $Nd_3Ni_{13}B_2$-type structure is investigated by a high temperature disturbance using molecular dynamics. We thus performed molecular dynamics simulations at constant pressure and temperature (NPT) with a 5×5×5 periodic super-cell. For constant-NPT molecular dynamics the temperature and pressure are maintained constant using an extended system[31] with a thermostat and barostat relaxation time of 0.1 ps. The simulation temperatures are 100, 295 and 503 K, respectively. For each temperature and at 1 atm (1 atm=1.01325×10^5 Pa). Pressure calculations are performed for 30000 steps with a time step of 2.0×10^{-15} s. After reaching equilibrium, the crystal symmetry retains the initial $P6/mmm$ space group at different temperatures. Lattice constants (Table 1) are found to be close to the experimental values and the phase stability is thus verified.

4. Phonon density of states of $R_3Ni_{13}B_2$

Phonon density of states (DOS) reflects the lattice dynamic properties, from which some important thermodynamic parameters can be derived. In this section, the lattice dynamic properties of $R_3Ni_{13}B_2$ (R=Y, Nd and Sm) intermetallics are firstly studied at an atomistic level using the inverted interatomic potentials. Figure 3 shows computed results by considering the contribution to the DOS of the distinct atoms. It can be seen from the total DOS that the highest frequencies of intermetallics $R_3Ni_{13}B_2$ (R=Y, Nd and Sm) are 15.55, 14.54 and 14.72 THz, respectively. For every spectrum, it can be divided into two parts at about 9.95, 9.22 and 9.36 THz, respectively, where the phonon density is almost zero. The second part is called high frequency localized modes. From the partial DOS, it can be inferred that the vibrational modes are mostly excited by Ni and B atoms in the high frequency and high frequency localized modes.

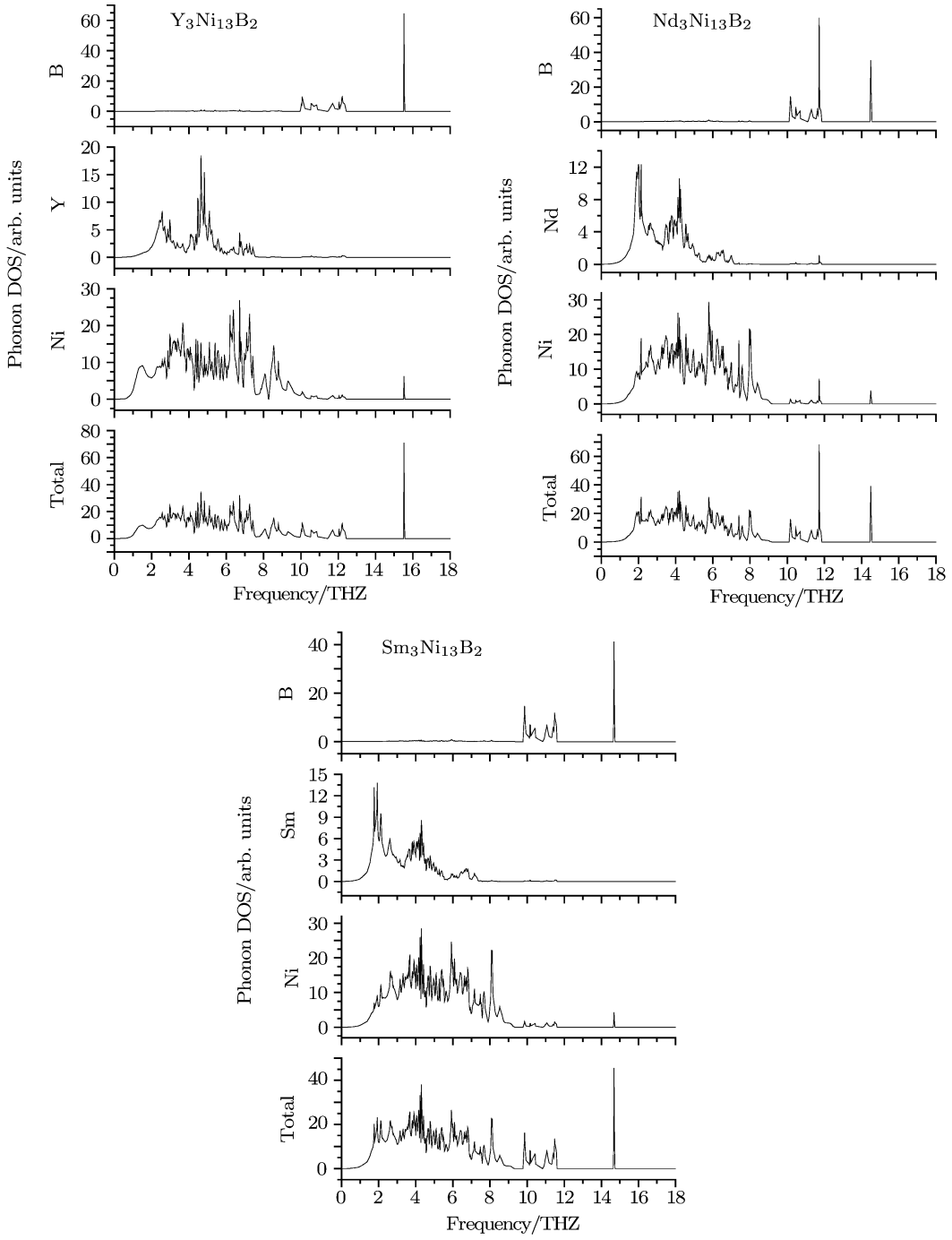


Fig. 3. Phonon densities of states of $R_3Ni_{13}B_2$.

However, B only contributes to the modes above 9.98, 10.12 and 9.80 THz for R=Y, Nd and Sm, respectively. In the range 0–10 THz, the vibrational modes are mostly excited by Ni atoms. The R atoms only contribute to modes below 7.00 THz.

One can analyse qualitatively the modes from interaction potentials by only considering the neighbours in Fig. 1. We choose R=Sm as an example in $R_3Ni_{13}B_2$ systems. For $Sm_3Ni_{13}B_2$ six Ni atoms are presented at the 6i site and eight B atoms are at the 2c sites around Sm (1a). There are six Ni atoms at 3g site and eight Ni atoms at the 4h sites around Sm (2e). Distances between Sm (1a)–Ni (6i), Sm (1a)–B (2c), Sm (2e)–Ni (3g) and Sm (2e)–Ni (4h) are 3.09, 2.91, 3.21 and 2.91 Å (1 Å=0.1 nm), respectively. Figure 1 shows that Sm reacts strongly with Ni and B at these distances. The mass of Sm is much larger than that of Ni and is thus assumed to be motionless relative to the Ni or B atom. Some Ni or B atoms are restricted to the 'potential well' $\Phi_{\mathrm{Sm-Ni}}(r)$ or $\Phi_{\mathrm{Sm-B}}(r)$. This might be the reason for the appearance of Ni or B localized modes corresponding to the higher transected frequency. The Sm atoms only contribute to lower frequency vibrations in the Sm–Ni or Sm–B 'potential well' because of their large atomic mass. If we choose the Ni atom at the 6i sites as a centre, there are two B atoms, two Ni atoms at the 4h sites and four Ni atoms at the 6i sites around. The distances between Ni (6i)–B(2c), Ni (6i)–Ni (4h) and Ni (6i)–Ni (6i) are 2.40, 2.49 and 2.53 Å, respectively. From Fig. 1, it can be seen that Ni reacts strongly with Ni or B at these distances. The very strong interaction between Ni and Ni at their neighbouring distance causes Ni to contribute a major part in the range 0–10 THz. On the other hand, the mass of Ni is approximately four times larger than that of B, so Ni is assumed to be motionless relative to B atom. Consequently, B atom restricted by Ni, which makes it in the 'potential well' Ni–B, excites some local modes. For B atoms, the optic modes are far separated from the acoustic modes and have very high frequencies which are due to the large mass difference in the atoms and the strong force constants between nearest neighborus Ni or Sm and B atoms.

In addition to the DOS, we have calculated the Debye temperature from our obtained results by lattice dynamic data as a function of temperature. The Debye temperature of a material is a suitable parameter to describe phenomena of solid-state physics which are associated with lattice vibrations. In our calculation, the lattice specific heat, C_V, is straightforwardly obtained from

$$C_V(T) = 3Nk_{\mathrm{B}} \int_0^{\infty} \frac{(\hbar\omega/k_{\mathrm{B}}T)^2 \mathrm{e}^{\hbar\omega/k_{\mathrm{B}}T}}{(\mathrm{e}^{\hbar\omega/k_{\mathrm{B}}T}-1)^2} g(\omega)\mathrm{d}\omega,$$

where $g(\omega)$ is total DOS. In the conventional Debye model, the Debye temperature Θ_{D} can be defined by $\hbar\omega_m = k_{\mathrm{B}}\Theta_{\mathrm{D}}$. The specific heat can be written as

$$C_V = 3Nk_{\mathrm{B}}(T/\Theta_{\mathrm{D}})^3 \int_0^{\Theta_{\mathrm{D}}/T} \frac{x^4 \mathrm{e}^x}{(\mathrm{e}^x-1)^2}\mathrm{d}x, \quad (1)$$

where $x = \hbar\omega_m/k_{\mathrm{B}}\Theta_{\mathrm{D}}$, k_{B} represents Boltzmann constant, $\hbar$ represents Planck constant and N represents the number of atoms in each cell. In the Debye model, ω_m is determined by

$$\int_0^{\omega_m} g(\omega)\mathrm{d}\omega = 3N\,,$$

that is, the integral is performed in the complete phonon DOS. Figure 4 shows the variation of the Debye temperature with temperature from 0 to 300 K. The Debye temperatures of $R_3Ni_{13}B_2$ are 442, 398 and 395 K at near 0 K for R=Y, Nd and Sm, respectively. As a last point, due to non-availability of the experimental values, we could not compare our results on DOS. And this makes it possible to predict some properties related to lattice vibration.

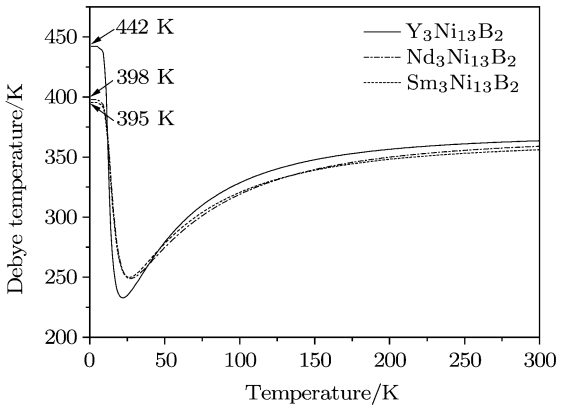


Fig. 4. Calculated Debye temperature of $R_3Ni_{13}B_2$.

5. Conclusion

Pair potentials based on *ab initio* calculations and on the lattice-inversion method have been used to calculate the structural properties of the $R_3Ni_{13-x}Co_xB_2$

(R=Y, Nd and Sm) series of compounds. The results show that Co substitution for Ni in $R_3Ni_{13-x}Co_xB_2$ causes the cohesive energy of the crystal to decrease and Co preferentially occupies the 3g site. The calculated lattice parameters coincide well with experimental values. It is noteworthy that the interatomic potentials are successfully used to calculate the vibrational properties of rare earth compounds $R_3Ni_{13}B_2$, which is important for future work on research and prediction of material structure.

Acknowledgements

The authors would like to thank professors F. M. Yang and J. K. Liang at Institute of Physics of the Chinese Academy of Sciences for interesting discussion and encouragement.

References

[1] Luo H Z, Jia L, Li Y X, Meng F B, Shen J, Chen N X, Wu G H and Yang F M 2005 *Acta Phys. Sin.* **54** 5246 (in Chinese)

[2] Gong Y M, Lan Z H, Yan Y, Du X B, Wang W Q, Wang X F, Su F, Lu L, Zhang Z S, Jin H M and Wen G H 2008 *Chin. Phys.* B **17** 1130

[3] Meng F B, Guo H J, Liu G D, Liu H Y, Dai X F, Luo H Z, Li Y X, Chen J L and Wu G H 2009 *Chin. Phys.* B **18** 3031

[4] Wang W Q, Xu S F, Xu Q Y, Zhang W L and Chen D F 2006 *Acta Phys. Sin.* **55** 3531 (in Chinese)

[5] Chen Y and Shen J 2009 *Acta Phys. Sin.* **58** S141 (in Chinese)

[6] Strnat K J and Strnat R M W 1991 *J. Magn. Magn. Mater.* **100** 38

[7] Hadjipanayis G C 1999 *J. Magn. Magn. Mater.* **200** 373

[8] Rhodes P and Wohlfarth E P 1963 *Proc. R. Soc. Lond.* Ser. A **273** 247

[9] Uebayashi K, Terao K and Yamada H 2002 *J. Alloys Compounds* **346** 47

[10] Kuz'ma Yu V and Bilonizhko N S 1981 *Dopov. Akad. Nauk. Ukr. RSR* Ser. A: *Fiz.-Mat. Tekh. Nauki* **10** 87

[11] Kuz'ma Yu B, Bilonizhko N S, Chaban N F and Chernyak G V 1983 *J. Less-Common Met.* **90** 217

[12] Chen Y, Liu Q L, Liang J K, Chen X L, Shen B G and Huang F 1999 *Appl. Phys. Lett.* **74** 856

[13] Chen Y, Li X, Chen X L, Liang J K, Rao G H, Shen B G, Liu Q L, Jin L P and Wang M Z 2000 *Chem. Mater.* **12** 1240

[14] Rillo C, Arauzo A, Plugaru N, Hlil E K, Rubín J and Bartolomé J 2007 *J. Magn. Magn. Mater.* **316** 166

[15] Bartolomé J, Plugaru N, Campo J, Rubín J, Hlil E K, Rillo C and Arauzo A 2007 *J. Alloys Compd.* **442** 11

[16] Plugaru N, Rubín J and Bartolomé J 2005 *Phys. Rev.* B **71** 024433

[17] Plugaru N, Rubín J, Bartolomé J and Piquer C 2005 *J. Magn. Magn. Mater.* **290–291** 1564

[18] Plugaru N, Rubín J, Bartolomé J, Campo J, Cuello G J, Tovar M and Prokhnenko O 2007 *J. Magn. Magn. Mater.* **316** e438

[19] Parthe E and Chabot B 1984 *Handbook on the Physics and Chemistry of Rare Earths* (Amsterdam: Elsevier Science) Vol. 6 p. 113

[20] Qian P, Chen N X and Shen J 2005 *Solid State Commun.* **134** 771

[21] Chang H, Chen N X, Liang J K and Rao G H 2002 *J. Phys: Condens. Matter* **14** 1

[22] Shen J, Qian P and Chen N X 2005 *Model. Simul. Mater. Sci. Eng.* **13** 239

[23] Chen N X, Shen J and Wang X L 2003 *J. Alloy Compd.* **359** 91

[24] Li W X, Cao L Z, Shen J, Chen N X, Liu B D, Wang J L, Wu G H, Yang F M and Li Y X 2003 *J. Appl. Phys.* **93** 6921

[25] Tian H J, Qian P, Shen J and Chen N X 2008 *Comput. Mater. Sci.* **44** 702

[26] Qian P, Wang Q L, Chen N X and Shen J 2006 *J. Phys.* D: *Appl. Phys.* **39** 1197

[27] Chen N X and Ren G B 1992 *Phys. Rev.* B **45** 8177

[28] Chen N X, Chen Z D and Wei Y C 1997 *Phys. Rev.* E **55** R5

[29] Shen J, Wang Y, Chen N X and Wu Y 2000 *Prog. Nat. Sci.* **10** 502

[30] Ni X D, Chen N X and Shen J 2001 *J. Mater. Res.* **16** 344

[31] Melchionna S, Ciccotti G and Holian B L 1993 *Mol. Phys.* **78** 553